Sub cycle Corrosion fatigue Crack Growth under Variable Amplitude Loading

by

Bianca Kurian

A Thesis Presented in Partial Fulfillment
of the Requirements for the Degree
Master of Science

Approved July 2019 by the
Graduate Supervisory Committee:

Yongming Liu, Chair
Qiong Nian
Houlong Zhuang

ARIZONA STATE UNIVERSITY

August 2019

ABSTRACT

Corrosion fatigue has been of prime concern in railways, aerospace, construction industries and so on. Even in the case of many medical equipment, corrosion fatigue is considered to be a major challenge. The fact that even high strength materials have lower resistance to corrosion fatigue makes it an interesting area for research. The analysis of propagation of fatigue crack growth under environmental interaction and the life prediction is significant to reduce the maintenance costs and assure structural integrity. Without proper investigation of the crack extension under corrosion fatigue, the scenario can lead to catastrophic disasters due to premature failure of a structure. An attempt has been made in this study to predict the corrosion fatigue crack growth with reasonable accuracy. Models that have been developed so far predict the crack propagation for constant amplitude loading (CAL). However, most of the industrial applications encounter random loading. Hence there is a need to develop models based on time scale. An existing time scale model that can predict the fatigue crack growth for constant and variable amplitude loading (VAL) in the Paris region is initially modified to extend the prediction to near threshold and unstable crack growth region. Extensive data collection was carried out to calibrate the model for corrosion fatigue crack growth (CFCG) based on the experimental data. The time scale model is improved to incorporate the effect of corrosive environments such as NaCl and dry hydrogen in the fatigue crack growth (FCG) by investigation of the trend in change of the crack growth. The time scale model gives the advantage of coupling the time phenomenon stress corrosion cracking which is suggested as a future work in this paper.

DEDICATION

To my parents who strengthen me with their love and care.

To my family who made my life colorful and joyful even in tough times.

To my teachers who moulded me into a knowledgable person.

To my friends who always cheered on me in my life journey.

To everyone who helped me reach where I am.

ACKNOWLEDGMENTS

I would like to express my gratitude to my faculty advisor Dr. Yongming Liu, for his guidance and support throughout my research work and for his suggestions that made this a better work. I would like to thank my committee members, Dr. Houlong Zhuang, Qiong Nain for their valuable comments and for their effort to review this work. I would also like to thank Karthik Rajan Venkateswaran, PhD student at Arizona State University for throwing some light onto my work.

Above, all I thank Almighty God for guiding me and strengthening me through my difficult times.

TABLE OF CONTENTS

Page

LIST OF TABLES

Table Page

TABLE OF FIGURES

Figure Page

CHAPTER 1
INTRODUCTION

Corrosion fatigue has been of prime interest for decades in various industrial applications. Researches have been conducted to study the behavior of materials under different environments to develop various models for the prediction of life of structures. Developing a model for the prediction of fatigue crack growth in aggressive environments reduce the possibility of premature failure that might happen without considering the environmental interactions with fatigue loading.

In the first chapter, a brief introduction to the ideas of fatigue loading and corrosion fatigue is presented. Different crack propagation models developed for constant amplitude loading are discussed in detail. Various factors affecting corrosion fatigue is studied to analyze the significance of these parameters. In the second chapter, an existing time scale model that predicts the fatigue crack growth in the Paris region is improved to extend the prediction to near threshold region for various alloys under any type of loading condition. The third chapter presents the work done to improve the model to account for the change in fatigue crack growth rate under environmental interactions with fatigue loading. Mainly two types of corrosion are considered in the development of the model which is discussed in detail. The modified model is validated against the experimental data collected from literature in their corresponding chapters. The final section is concluded with the findings from this study. It gives a scope of the work that may be carried out in the future.

1.1. Background and literature review

1.1.1. Introduction to Fatigue Loading

A structure may fail at stress below the ultimate tensile strength or even the yield point due to repeated loading. This is due to the progressive failure by initiation and propagation of cracks that grow to an unstable size (fatigue). This is termed as fatigue failure. This type of failure usually occurs with no/ little warning if the crack goes unnoticed. The fatigue failure occurs in three stages: 1) Crack Initiation 2) Crack Propagation and 3) Failure. Researches have been going on to analyze the crack propagation to predict the failure of material. When a load is applied on a structure, the stress concentration is not uniform and is more at the crack tip compared to any undamaged area of the structure. The cracks might have been introduced in the structure as manufacturing defect or might have initiated due to fatigue loading. The stress distribution ahead of the crack tip due to the applied load is represented in terms of stress intensity factor, which causes the crack to grow. It is given as,

$$K = Y\sigma\sqrt{\pi a} \quad (1)$$

The geometric correction factor Y is a function of the crack length and width W of the specimen and hence is geometry dependent. The stress intensity range due to the applied stress range is defined as

$$\Delta K = Y\Delta\sigma\sqrt{\pi a} \quad (2)$$

According to Sadananda and Holtz [1], a two-parameter model is chosen to be the crack tip driving force wherein K_{max} and ΔK are intrinsic to fatigue growth. The crack

growth rate as a function of stress intensity range is represented in a logarithmic scale. Based on the crack propagation rates, it is divided into three regimes as shown in Figure 1. In regime A (Near Threshold region), the propagation rates are of the order 10^{-9} m/cycle or less. The crack growth is negligible or is nearly zero for stress intensity range below ΔK_0. ΔK_0 is the threshold stress intensity range above which there is a visible crack growth. In regime B (Paris regime), the propagation rates are of the order of $10^{-9} – 10^{-6}$ m/cycle and the crack growth is linear. In regime C, the crack grows in an asymptotic way and the material fractures at critical stress intensity, K_c

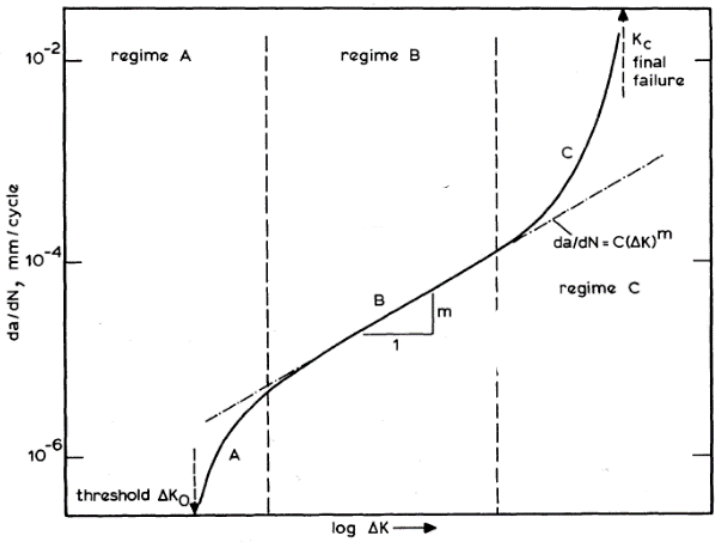

Figure 1. Fatigue crack growth rate curve. Log-log graph for da/dN vs ΔK

With increase in stress ratio, $= \frac{\sigma_{min}}{\sigma_{max}}$, the threshold decreases and crack growth rates are faster compared to low R ratios.

1.1.1.1. Different Crack Propagation Models for Fatigue Loading

Various fatigue crack propagation models were developed for constant amplitude fatigue loading. In a constant amplitude loading, all the load cycles are identical with same peak stress, range of applied stress, mean stress and stress ratio.

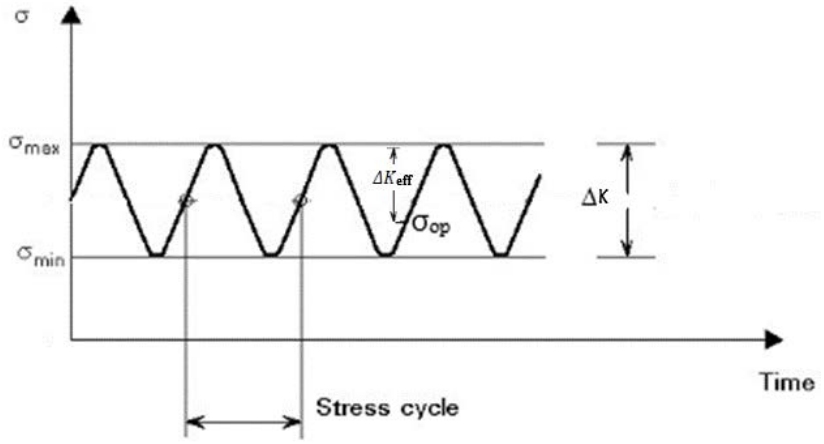

Figure 2. Constant amplitude loading

Paris [2] developed a crack propagation model for second regime as

$$\frac{da}{da} = C\Delta K^m \tag{3}$$

C and m are Paris constant obtained from experimental data. C and m are the intercept and slope of Paris regime respectively. The limitation of this model is that it does not predict the growth in the near threshold and the critical growth region. It does not take into account the effect of Ratio. Forman [1967] [3] modified this equation to incorporate R effect and the growth in in region 3 as

$$\frac{da}{dn} = C\frac{\Delta K^n}{(1-R)K_{IC} - \Delta K} \tag{4}$$

Nicholson [1973] [4] proposed a model that incorporates the crack growth rate in the near threshold regime as well

$$\frac{da}{dn} = A\frac{(\Delta K - \Delta K_{th})^n}{K_{IC} - K_{max}} \tag{5}$$

Elber [1970] [5] introduced the concept of crack closure that explained the effect of R ratios on the fatigue crack growth rates. The crack closure is a result of the crack tip plasticity. He argued that crack remain closed until a certain stress level (opening stress σ_{op}) is reached. σ_{op} is usually higher than the minimum stress σ_{min}. Below $\sigma_{op,}$ the crack does not propagate. With higher R, the closure level is reduced inducing faster growth rates. The effective stress intensity range $\Delta K_{eff} = K_{max} - K_{op}$ is used in calculating the fatigue crack growth. Khan [6] developed a model that calculates the crack increment as a function of plastic zone ahead of the crack tip and is given as

$$\frac{da}{dn} = C\left(\frac{\Delta K_{eff}}{\sigma_{ys}}\right)^2\left(\frac{\Delta K - \Delta K_{th}}{K_{IC} - K_{max}}\right)^n \tag{6}$$

Wheeler [7] developed a crack tip plasticity based crack propagation model to calculate fatigue growth under the application of single overload as

$$\frac{da}{dn} = (C_p)_i[C(\Delta K)_i{}^m] \tag{7}$$

C_p is retardation parameter depending on the plastic zone size of i^{th} cycle and the overload plastic zone size. Newman [8] proposed that the opening stress σ_{op} varies for different stress

level. σ_{op} is calculated for different cycles. According to Bannantine [9], the crack propagation is calculated as

$$\frac{da}{dn} = A(\Delta K_{eff})^m \tag{8}$$

A is calculated from Paris constant C as

$$A = \frac{C}{(U_i)^m} \tag{9}$$

Where $U_i = \frac{\Delta K_{eff,i}}{\Delta K_{appl,i}}$

These models only predict the fatigue growth during a cycle and not at any arbitrary time. Lu and Liu [10] expressed the instantaneous crack growth rate at any arbitrary time point as

$$\dot{a} = H(\dot{\sigma}).H(\sigma - \sigma_{ref})\frac{2C\lambda\sigma}{1 - C\lambda\sigma^2}\dot{\sigma}.a \tag{10}$$

Where H(x) is the Heaviside function

$$H(x) = \begin{cases} 0, & x \leq 0 \\ 1, & x > 0 \end{cases}$$

This model can be used to predict the crack propagation in a variable amplitude loading where the load cycles are not identical as shown in Figure 3.

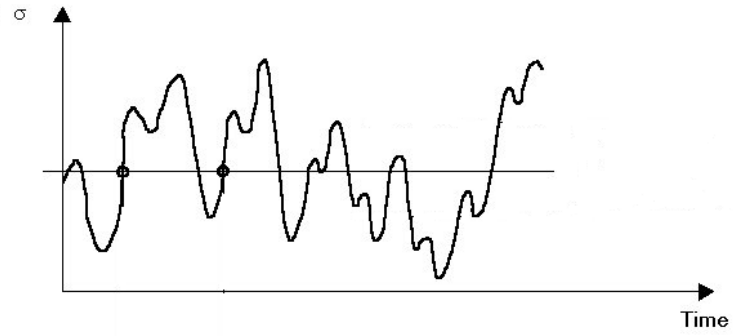

Figure 3. Variable amplitude loading

There are two hypotheses involved in the derivation of this small time scale formulation: 1) crack does not grow during unloading, 2) crack grows only during a part of the loading path. Zhang and Liu [11] verified these hypotheses through in situ testing and imaging analysis. They observed that no/very small crack growth occurred during unloading. They noticed that crack tip opens only when SIF exceeds certain loading level (σ_{ref}). The crack does not grow until this loading level. Once the crack tip starts to open, the crack starts to grow. The crack increment da within a cycle varied non-linearly with crack tip opening displacement δ

$$da \propto \sqrt{\delta} \tag{11}$$

Using a power function to fit the crack growth kinetics with respect to ctod variation, they expressed instantaneous crack growth rate function for Al 7075- T6 as

$$\frac{da}{dt} = \frac{AK_{max}^2}{2\sqrt{\delta}} \frac{d\delta}{dt} \tag{12}$$

Lu and Liu [12] introduced a model to estimate the ctod at an applied stress in a cyclic loading as

$$\delta = \begin{cases} \frac{K^2}{E\sigma_y} & K \geq K_{maxmem} \\ \delta_{min,m-1} + \frac{(K - K_{min,m-1})^2}{2E\sigma_y} & K_{max,m-1} \leq K < K_{maxmem} \\ \delta_{min,m} + \frac{(K - K_{min,m})^2}{2E\sigma_y} & K \leq K_{max,m-1} \end{cases} \quad (13)$$

For the unloading path, ctod at any applied stress is calculated as

$$\delta = \begin{cases} \delta_{min,m} - \frac{(K_{max,m} - K)^2}{2E\sigma_y} & K \geq K_{min,m-1} \\ \delta_{min,m-1} - \frac{(K_{max,m-1} - K)^2}{2E\sigma_y} & K < K_{min,m-1} \end{cases} \quad (14)$$

Later on, Karthik and Liu [13] modified the small time scale model to incorporate different types of alloys as

$$\Delta a = \frac{AK_{max}^B \Delta\delta}{\sqrt{\delta_i} + \sqrt{\delta_{i-1}}} \quad (15)$$

The change in ctod between two applied stresses, $\Delta\delta = \delta_{curr} - \delta_{prev}$

$$\begin{aligned} \delta_i &= \delta_{curr} - \delta_{min} \\ \delta_{i-1} &= \delta_{prev} - \delta_{min} \end{aligned} \quad (16)$$

A and B are the fitting parameters determined from the experimental data at R = 0.

1.1.1.2. Determination of crack opening stress for constant and Variable Amplitude Loading

The crack opening stress is a consequence of complex interaction of forward plastic zone created during loading path and reverse zone plastic zone created during the unloading path [14]. For positive stress ratio (tensile-tensile loading), unloading produces compressive residual stress ahead of the crack tip. This results in local crack closure near to the crack tip. This compressive residual stress needs to be reversed indicating the crack will grow after reaching σ_{ref}. In case of negative R ratio (tensile-compressive loading), during unloading the local crack closure happens and when it enters the compressive loading, a global crack closure happens far from the crack tip due to the applied compressive stress along with the local crack closure. During unloading of compressive stress, tensile residual stresses are generated ahead of the crack tip and crack starts to open. While continuing to the tensile loading, the forward plastic zone aids in crack opening. Thus, the compressive loading reduces the crack opening stress level [15]. Karthik came up with an equation for opening stress, which is applicable for constant and variable amplitude loading. It is derived as follows [13]

$$d_{r,virtual} - d_r = d$$

$$\frac{\pi}{8}\left(\frac{\sigma_{max} - \sigma_{min}}{2\sigma_y}\right)^2 \pi(a-d)Y^2 - \frac{\pi}{8}\left(\frac{\sigma_{max} - \sigma_{cl}}{2\sigma_y}\right)^2 \pi a Y$$

$$= \frac{\pi}{8}\left(\frac{\sigma_{op} - \sigma_{min}}{\sigma_y}\right)^2 \pi Y^2 (a-d)$$

At $\sigma = \sigma_{op}$, $d = 0$

$$\frac{\pi}{8}\left(\frac{\sigma_{max}-\sigma_{min}}{2\sigma_y}\right)^2 \pi a Y^2 - d_r = \frac{\pi}{8}\left(\frac{\sigma_{op}-\sigma_{min}}{\sigma_y}\right)^2 \pi a y^2$$

$$r_{f,max} = \alpha\left(\frac{K}{\sigma_y}\right)^2 = \frac{\alpha\sigma_{max}^2 Y^2 \pi a}{\sigma_y^2}$$

$$\sigma_{max} = \left(\frac{r_f}{\alpha\pi a}\right)^{0.5}\frac{\sigma_y}{Y}$$

Sub (a) in (1)

$$\frac{\pi}{8}\left[\frac{\left(\frac{r_f}{\alpha\pi a}\right)^{0.5}\frac{\sigma_y}{y}-\sigma_{min}}{2\sigma_y}\right]^2 Y^2\pi a - d_r = \frac{\pi}{8}\left(\frac{\sigma_{op}-\sigma_{min}}{\sigma_y}\right)^2 \pi a y^2$$

Divide by $\frac{\pi^2 a y^2}{8}$

$$\left[\frac{\left(\frac{r_f}{\alpha\pi a}\right)^{0.5}\frac{\sigma_y}{y}-\sigma_{min}}{2\sigma_y}\right]^2 - \frac{8d_r}{\pi^2 a y^2} = \left(\frac{\sigma_{op}-\sigma_{min}}{\sigma_y}\right)^2$$

Multiply by σ_y^2 throughout

$$\left[\frac{\left(\frac{r_f}{\alpha\pi a}\right)^{0.5}\frac{\sigma_y}{Y}-\sigma_{min}}{4}\right]^2 - \frac{8\sigma_y^2 d_r}{\pi^2 a Y^2} = \left(\sigma_{op}-\sigma_{min}\right)^2$$

Take square root on both sides

$$\left\{\frac{1}{4}\left[\left(\frac{r_f}{\alpha\pi a}\right)^{0.5}\frac{\sigma_y}{\gamma}-\sigma_{min}\right]^2 - \frac{8\sigma_y^2 d_r}{\pi^2 a Y^2}\right\}^{0.5} = \sigma_{op}-\sigma_{min}$$

$$\sigma_{op} = \sigma_{min} + \left\{\frac{1}{4}\left[\left(\frac{r_f}{\alpha\pi a}\right)^{0.5}\frac{\sigma_y}{Y} - \sigma_{min}\right]^2 - \frac{8\sigma_y^2 d_r}{\pi^2 a Y^2}\right\}^{0.5}$$

$$= \sigma_{min} + \left\{\frac{1}{4}\left[\frac{\left(\frac{r_f}{\alpha}\right)^{0.5}\frac{\sigma_y}{Y} - \sigma_{min}\sqrt{\pi a}}{\sqrt{\pi a}}\right]^2 - \frac{8\sigma_y^2 d_r}{\pi^2 a Y^2}\right\}^{0.5}$$

$$= \sigma_{min} + \left\{\frac{1}{4}\left[\frac{\left(\frac{r_f}{\alpha}\right)^{0.5}\sigma_y - \sigma_{min}\sqrt{\pi a}Y}{\pi a Y^2}\right]^2 - \frac{8\sigma_y^2 d_r}{\pi^2 a Y^2}\right\}^{0.5}$$

$$= \sigma_{min} + \left\{\frac{1}{\pi a Y^2}\left[\frac{1}{4}\left(\left(\frac{r_f}{\alpha}\right)^{0.5}\sigma_y - \sigma_{min}Y\sqrt{\pi a}\right)^2 - \frac{8\sigma_y^2 d_r}{\pi}\right]\right\}^{0.5}$$

$$\sigma_{op} = \sigma_{min} + \frac{1}{Y}\left\{\frac{1}{\pi a}\left[\frac{1}{4}\left(\left(\frac{r_f}{\alpha}\right)^{0.5}\sigma_y - \sigma_{min}Y\sqrt{\pi a}\right)^2 - \frac{8\sigma_y^2 d_r}{\pi}\right]\right\}^{0.5} \quad (17)$$

1.1.2. Introduction to Corrosion Fatigue

Corrosion fatigue is the damage due to crack growth in a material undergoing cyclic loading in the presence of a corrosive media. Corrosion fatigue may accelerate or decelerate the crack growth rate. CFCP depends on various factors such as cyclic stress intensity, stress ratio, complex interaction of time and environmental variables [16]. Corrosion fatigue is mainly attributed to hydrogen embrittlement and anodic dissolution. The embrittlement of material occurs through decohesion, adsorption or hydride formation. The hydrogen atoms that enter the lattice reduce the cohesion forces among the atoms of

the material weakening the material. Surface energy is reduced due to the adsorption of hydrogen atoms making the material more energetically favorable for fracture in adsorption mechanism [17]. Hydride formation mechanism is characterized by the formation of hydrides at the crack tip making the material brittle. In anodic dissolution, the passive film within a crack initiated due to applied stress rupture exposing new surface to the corrosive environment. This surface gets partially dissolved facilitating the crack growth. Solutions with halide ions such as I, Br, Cl usually accelerates CFCP while nitrate inhibitors in chloride solution inhibit CFCP in aluminium alloys [18]. Ritchie, Suresh and Liaw [19] compared the fatigue growth behavior in high and low strength steels in dry gaseous hydrogen and moist air. They observed that in low strength alloys, which are resistant to hydrogen embrittlement, the crack growth rates seems to accelerate in hydrogen environment compared to moist air in contrary to what was expected. However, this influence was markedly visible only at low R ratios. High strength steels that are prone to hydrogen embrittlement showed retardation of crack growth in hydrogen environment irrespective of R ratios. At intermediate crack growth rates of 10^{-6} mm/cycle, crack propagation seems to be enhanced by hydrogen owing to hydrogen embrittlement.

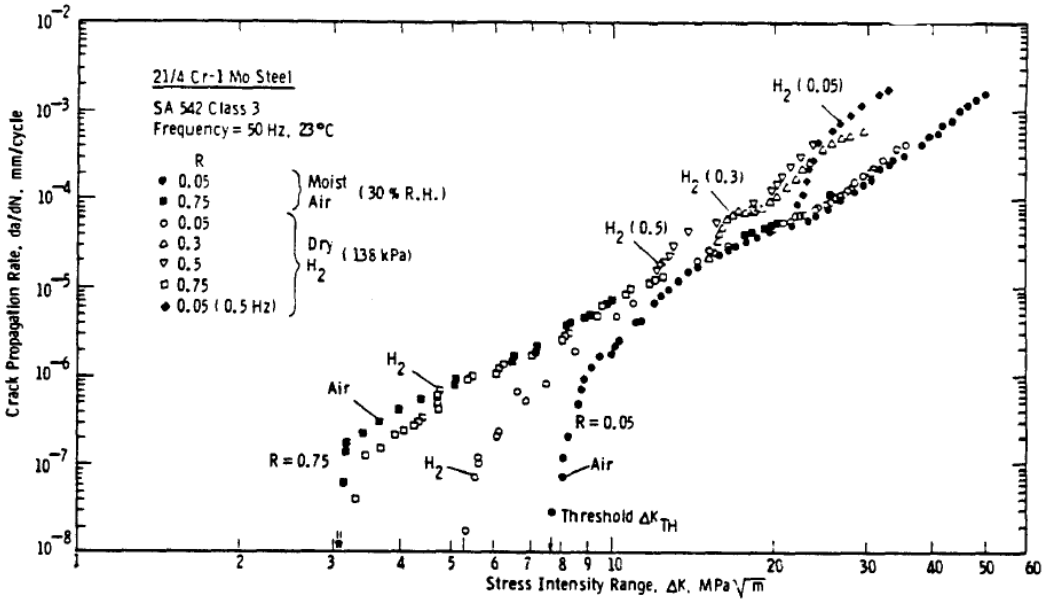

(a)

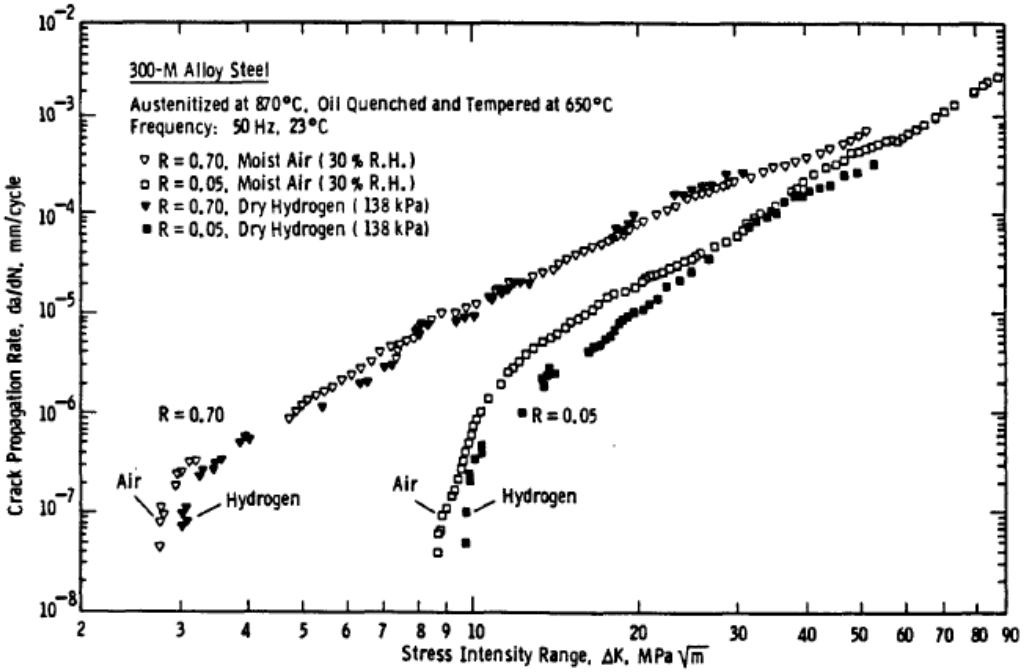

(b)

Figure 4: Effect of dehumidified hydrogen gas on fatigue crack propagation in a) lower strength 2 1/4 Cr-1Mo SA542-3 steel b) high strength 300-M steel [19]

1.1.2.1. Different Crack Propagation Models for Corrosion Fatigue

Wei and Landes [20] proposed a Linear Superposition Model in which that the crack growth rate in a corrosive environment is the sum of fatigue growth rate due to mechanical loading in inert environment and time based environmental crack growth rate

$$\frac{da}{dN_E} = \frac{da}{dN_M} + \frac{da}{dN_{SCC}} \tag{18}$$

The crack growth rate due to SCC is calculated by performing integration of crack growth data as function of the applied stress intensity factor

$$\frac{da}{dN_{SCC}} = \int_0^{1/f} \frac{da}{dt}(K)\,[K(t)]dt \tag{19}$$

For nickel based super alloys environment assisted crack growth rate reduces to

$$\frac{da}{dN_E} = \frac{da}{dN_M} + C(\Delta K)^n t_{eff} \tag{20}$$

t_{eff} is (1/f) in case of a square wave cycle. This model can be used only for those material/environment systems where MECP kinetics have a significant contribution to environmental assisted fatigue growth.

1.1.2.2. Factors affecting corrosion fatigue crack growth rate

Stewart [21] stated that environment influences fatigue crack growth rates with their effect depending on the environment under which the material is subjected to failure. The effect of environment is significant in the near threshold regime affecting the threshold

intensity values ΔK_{th} at different stress ratios. He observed that there is a decrease in growth rate in vacuum compared to air while the crack growth rate increases in dry environments (hydrogen, argon) at lower R ratios with ΔK_{th} being lower than that in air. At higher R ratios, ΔK_{th} is almost insensitive to the environment. Pao and Haltz [22] conducted experiment to study the effect of air, vacuum and NaCl on fatigue growth rate in the near threshold and Paris regimes in aluminum 7075 alloys. They studied the effect of these environments on ΔK_{th} as a function of R. It was clear from the experiment that fatigue growth rate in 1% NaCl is higher up to an order of magnitude compared to air even though ΔK_{th} in ambient air and 1% NaCl is comparable. The water vapor present in air reacts with crack surface and the hydrogen produced causes embrittlement that accelerates crack growth compared to vacuum. In the presence of NaCl, hydrogen embrittlement coupled with complex electrochemical reaction between NaCl and aluminium further accelerates the fatigue growth. In stage 1 region where the water/aluminium surface reactions are longest, the surface reactions are saturated in ambient air and salt water producing comparable hydrogen entry to the crack tip. This is the reason for similar ΔK_{th} in ambient air and 1% NaCl. They also figured out the effect of NaCl concentration on FCG. It was found that growth rate increase from 0.001% to 1% NaCl but remained almost same above 1%. ΔK_{th} remained same for all the concentration of NaCl.

Frederick and Gilbert [23] figured out the frequency effect on the fatigue crack propagation in aluminium alloy 2024 in NaCl environment. They observed that there is not much variation in the propagation rates from 2.5Hz – 10 Hz though the propagation rates are higher compared to that in air and distilled water. When the frequency is reduced to 1Hz, there is a decrease in propagation rate compared to 2.5Hz and higher frequencies,

while the propagation rates become closer to that in air and distilled water. When the frequency is further reduced to 0.1 Hz, FCGR retards and become comparable to that in air and distilled water. They concluded that rising time (RT) is the controlling factor rather than cycle period T. They conducted experiments with different types of waveform such as sinusoidal, positive saw tooth form and negative saw tooth form. They found that at 1Hz frequency, negative saw tooth form with less RT had higher growth rate while positive saw tooth form with highest RT has the least growth rate. At 5 Hz, they observed that the effect of corrosion on crack propagation saturates and all the waveforms showed comparable FCGs. They proposed that at short RT, there is localized dissolution and concomitant hydrogen production wherein the hydrogen atoms are taken to the crack tip resulting in embrittlement process. However, at higher RT, the crack tip surfaces are passivated during large amount of plastic deformation that hydrogen production is reduced. Hence hydrogen embrittlement could not produce significant effect on FCG. They also summarized that FCGR does not depend on the duration of exposure to corrosive medium. It was observed that crack growth rate per cycle is frequency independent in vacuum and moist air for frequencies under 50Hz in case of aluminium alloys. However, 7075 and 7079 alloys showed a frequency dependency below 10^{-3} and 1 Hz respectively in chloride solution [22]. It is characterized as

$$\frac{da}{dn} \propto f^{-\beta} \tag{21}$$

β is of the order of 0.5 in case of 7017 and 7045 and 0.1 for 7075 below 10^{-3} Hz.

Pao and Holtz stated that fatigue growth rate is influenced by frequency in moist air while in water and salt water, little or no frequency effect is observed. Sivaprasad [24]

observed inverse effect of frequency on fatigue growth. He conducted experiments on HSLA to find the behavior of steel in air and 3.5%NaCl. He found that FCG at 0.1Hz in NaCl is faster than FCG at 1Hz in NaCl for $\Delta K > 18$ MPa$\sqrt{m}$ while FCG slows down for $\Delta K < 18$ MPa$\sqrt{m}$

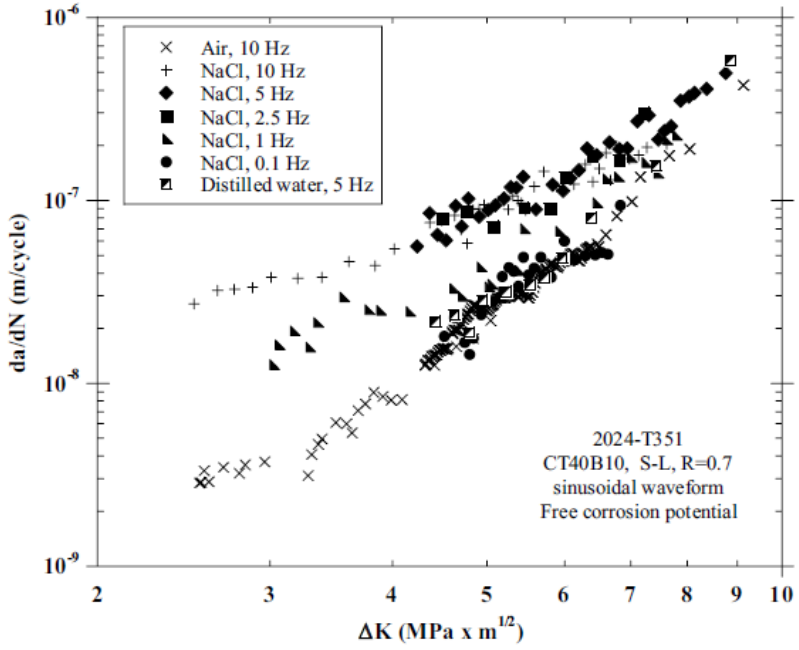

Figure 5. Effect of frequency on FCG of 2024-T351 steel [23]

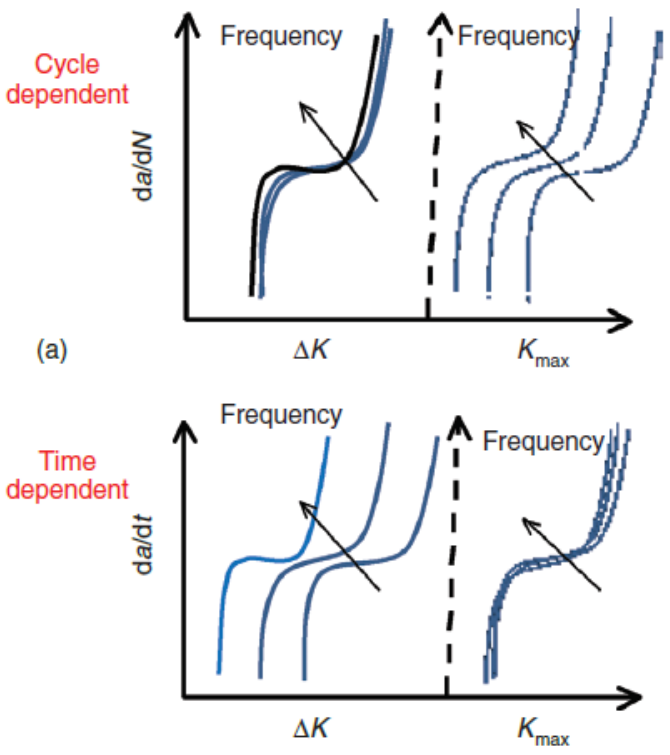

Figure 6. Effect of frequency on the propagation of crack in fatigue loading [29]

CHAPTER 2
NEAR THRESHOLD FATIGUE CRACK GROWTH MODEL

2.1. Overview

Determining the near threshold fatigue crack growth data is an important aspect in predicting the structural fatigue life. Mainly, there are two methods used to generate the fatigue crack growth data, load reduction method and CPCA method.

2.1.1. Load Reduction Method

Based on the ASTM standard E – 647 [25], a high ΔK is applied to initiate a crack at the notch and is reduced by 5% of applied load, maintain a constant R ratio for every 0.5mm of crack growth until the threshold condition (ΔKth) is reached. Once the threshold is reached, the load is increased to generate the crack growth curve in the near threshold and higher crack growth regions. Even though this test procedure has been used for a wide variety of materials for past few years, the method overestimate the threshold causing over prediction of life of the structure in turn leading to premature failure of the component. This method also produces remote closure creating large differences between small and large cracks than expected [26].

2.1.2. Compression-Compression Pre-cracking Constant-Amplitude Method (CPCA)

In CPCA method, the notched compact tension specimen, C(T) is loaded under compression-compression pre-cracking sequence until the crack grows to 0.25 – 0.5 mm.

Once the crack reaches the maximum extension, the crack stops growing further. A constant amplitude tension loading is then applied where the crack starts growing further. It needs to be ensured that the crack length is 2 – 3 times the compressive plastic zone so that the data will not be influenced by the tensile residual stresses at the notch. The CPCA method generates steady state constant amplitude curves minimizing the load history effect. Figure 7 shows CPCA loading sequence

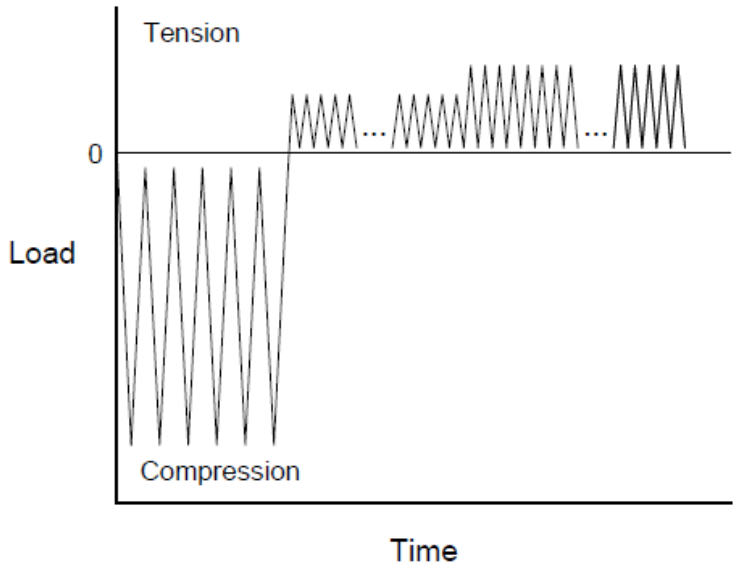

Figure 7. CPCA Loading Sequence [26]

2.2. Model Development of Fatigue Crack Growth rate for Near Threshold regime

The small time scale model developed by Karthik and Liu [13] predicts the fatigue crack growth over the Paris regime. It does not account for the lower crack growth rates in the near threshold regime and the unstable crack growth in the failure region. In order to estimate the crack growth in these two regions along with the Paris region, the time scale model is modified as

$$\dot{a} = H(\sigma_{eff} - \sigma_{th}) \frac{A K_{max}^{B}}{\sqrt{\delta}} \dot{\delta} \quad (22)$$

Where H(x) is the Heaviside function.

Equation () suggests that the crack does not grow until the threshold is reached. This does not mean that the crack grows for the entire loading cycle after the threshold is reached. It grows only during a portion of the applied loading cycle from σ_{op} to σ_{max}. A power law function is proposed to be incorporated in the small time scale model as

$$a = C_{th} A K_{max}^{B} \sqrt{\delta} \quad (23)$$

where C_{th} is the power law function to include the dependence of crack growth on the threshold condition and the fracture toughness of the material. For a constant amplitude loading, the power law function is expressed as

$$C_{th} = \left(\frac{\Delta K_{eff} - \Delta K_{th}}{K_{IC} - K_{max}} \right)^{n} \quad (24)$$

C_{th} takes care of the two extreme cases. When K_{max} approaches K_{IC}, the crack growth becomes unstable and at this point, the material failure occurs. When the stress intensity range approaches the threshold values, the crack grows in an asymptotic manner and becomes zero when it reaches ΔK_{th}. In case of variable amplitude fatigue loading (VAL), cycles are not well defined. A cycle may consist of many sub cycles for a VAL. In addition, the stress ratio cannot be defined, as it can be different for different cycles constituting the VAL. The maximum applied stress and the applied stress range varies for different cycles as well as the sub cycles. This makes it to define ΔK_{th} for a VAL. Since the change in ΔK_{th} with R ratio is attributes the crack closure effect, ΔK_{th} can be expressed in term of the

maximum monotonic plastic zone size and reverse plastic zone size. When a crack is unloaded from the maximum tensile stress, a reverse plastic zone of size d_r with compressive residual stress acting on the zone is formed at the crack tip as shown in Figure 8. This residual stress is transferred to the crack surfaces causing the crack surfaces to be closed fully or partially through a distance d. The crack propagates only when it is fully open. During reloading, the crack starts opening from σ_{min} to σ_{op}. It starts growing when the stress exceeds the opening stress

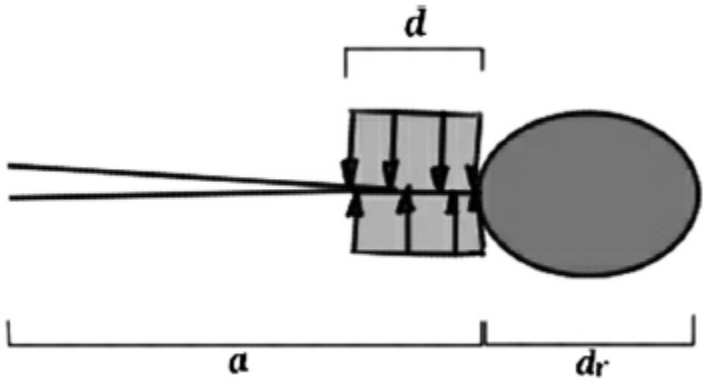

Figure 8. Reverse plastic zone and crack closure

If an overload is applied, the compressive residual stress generated is higher in magnitude and the crack opening stress is increase when crack enters this higher magnitude compressive region. When the crack is reloaded from minimum stress, a forward plastic zone of size r_f is formed at the crack tip. The crack opening stress attains a steady state when the current plastic zone reaches the boundary of the largest monotonic plastic zone as shown in Figure 9 [13].

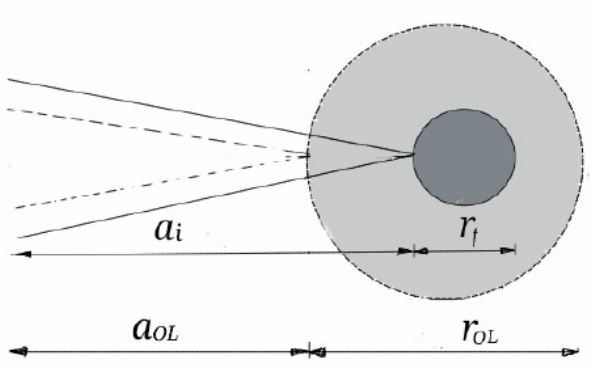

Figure 9. Monotonic plastic zone size

This closure effect is predominant in near threshold region [27] due to which ΔK_{th} decreases with increasing R. The variation of ΔK_{th} with respect to R is assumed to be a linear variation in case if alloys. This assumption is used in developing the near threshold fatigue crack growth model for VAL.

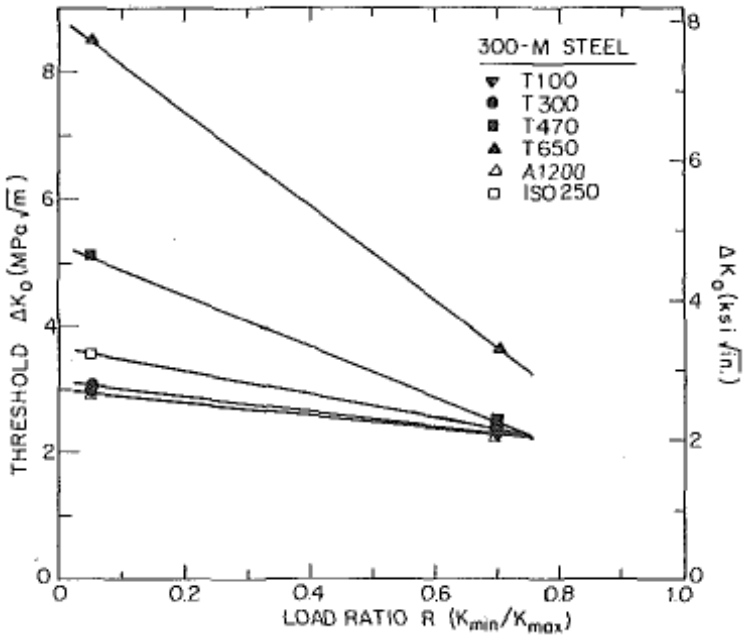

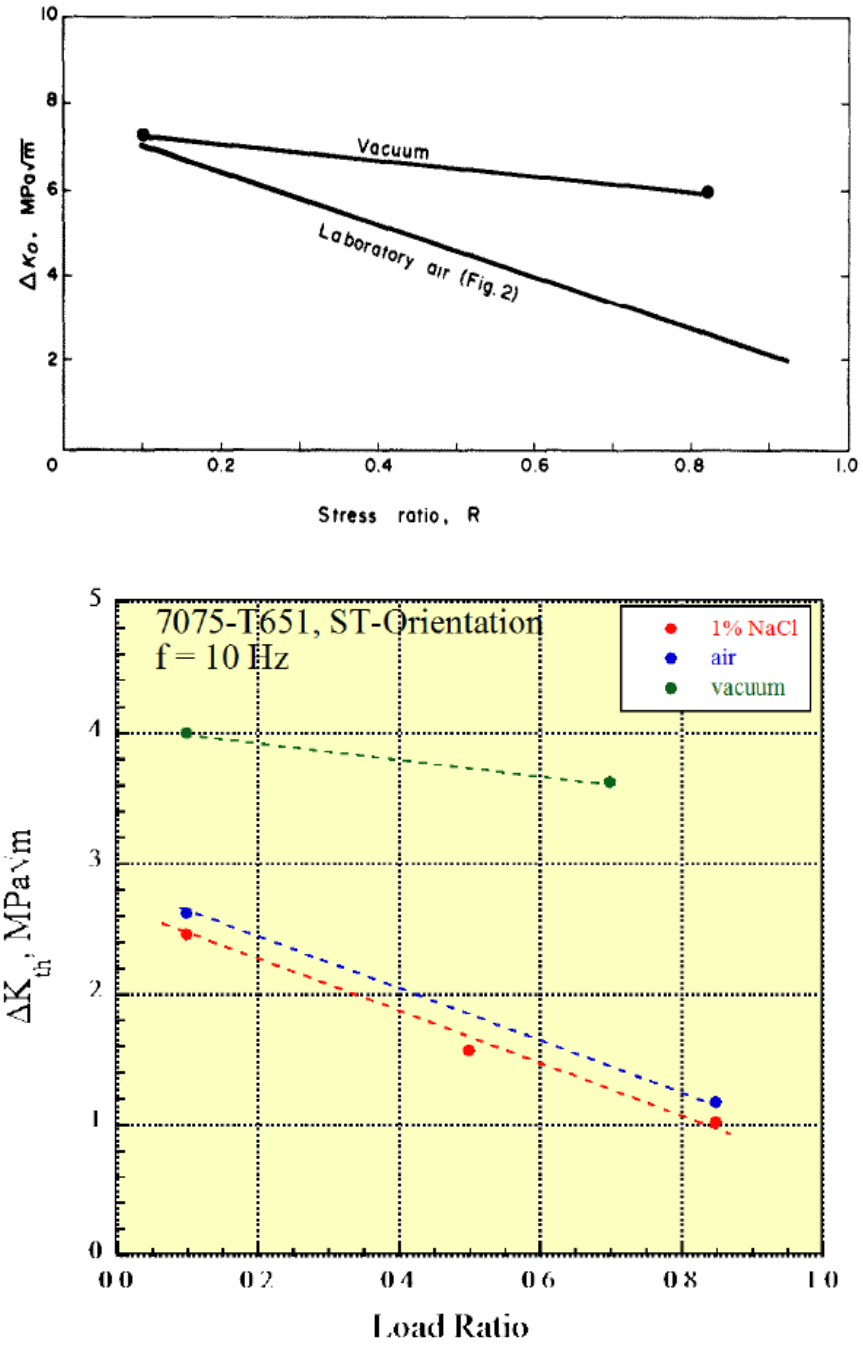

Figure 10. Stress intensity threshold (ΔK_{th}) vs load ratio R for a) 300M [27] b) 2NiCrMoV steel [19] c) Al 7075-T651 [22]

Using this linear relationship,

$$\Delta Kth = P - QR \tag{25}$$

P is the intercept and Q is the slope of the linear curve determined from ΔK_{th} vs R curve. Since R cannot be defined for a variable amplitude loading, R is expressed in terms of the plastic zone sizes.

$$R = \frac{K_{min}}{K_{max}} = 1 - \frac{\Delta K}{K_{max}} \tag{26}$$

According to Rice, the reverse plastic zone is expressed as

$$d_r = \frac{\pi}{8}\left(\frac{\Delta K}{2\sigma_y}\right)^2 \tag{27}$$

According to Dugdale model, the maximum monotonic plastic zone is

$$r_f = \frac{\pi}{8}\left(\frac{K_{max}}{\sigma_y}\right)^2 \tag{28}$$

From (27) and (28)

$$\frac{\Delta K}{K_{max}} = \sqrt{\frac{4r_f}{d_r}} \tag{29}$$

From (25), (26) and (29)

$$C_{th} = \left(\frac{\Delta K - (P - (Q(1 - \sqrt{\frac{4r_f}{d_r}})}{K_{IC} - K_{max}}\right)^n \tag{30}$$

n was determined empirically to be a very small value in case of constant as well as random loading. This generic equation can be used for both types of loading. The model validation can be found in chapter 4.

CHAPTER 3
MODEL DEVELOPMENT FOR CORROSION FATIGUE CRACK GROWTH

3.1 Overview

Vasudevan and Sadananda [1] proposed a two-parameter approach to quantify the fatigue crack growth data. They proposed that the two intrinsic thresholds ΔK_{th} and $K_{max,th}$ needs to be exceeded simultaneously for the fatigue crack to grow. They argued that the K_{max} is the controlling parameter for environmental interactions. They represented the threshold data, ΔK vs K_{max} as an L shaped curve with the two limiting values corresponding to the fundamental threshold. In case of pure fatigue, $\Delta K^* = K_{max}^*$ and hence for any crack growth rate the plot of ΔK^* vs K_{max}^* gives a straight line. Any deviations from the ideal fatigue behavior is characterized by larger K_{max}^* compared to ΔK^*. He classified the environmental effect on fatigue crack growth based on this curve into four types as shown in the below figure.

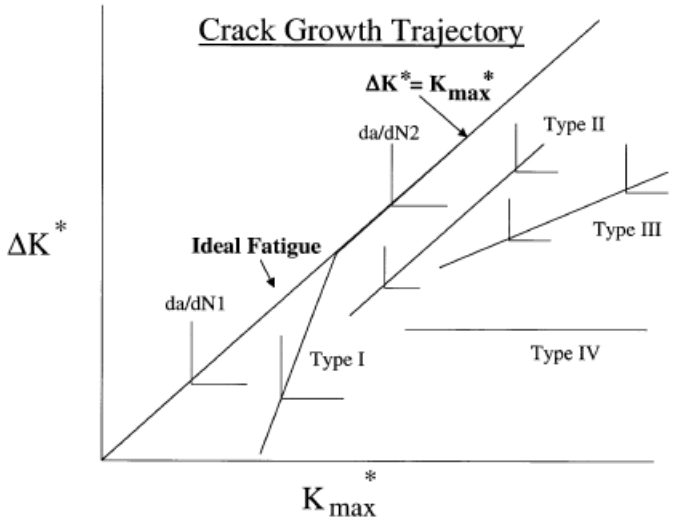

Figure 11. Classification of environmental interaction on fatigue crack growth rate on ΔK^* vs K_{max}^* [1]

Type I shows that aggressive environmental effect has major influence in the near threshold region. In Type II, the fatigue crack growth rate is affected due to environmental interactions at higher crack growth rates while it remains unaffected at lower crack growth rate. This effect is seen to be a parallel shift in the crack growth rate in the log-log plot of da/dN vs ΔK. The crack growth seems to have an accelerating effect in the Paris regime due to the fatigue loading in corrosive environment. The environmental effect is independent of K_{max} or transient time in this type of corrosion. They suggested that this type of corrosion is a consequence of rapid saturation of environmental effect with respect to the crack advance times providing a constant environmental contribution. The instantaneous covering of newly created surfaces with gaseous atoms or the continuous reaction and passivation and breaking of bonds can be the possible reasons for environmental saturation effect. Type III shows stress-driven environmental effects which is a characteristic of stress corrosion fatigue process while Type IV is an extreme case of Type III.

It can be seen from the literature that based on fatigue crack growth rate curve $\frac{da}{dN}$ vs ΔK, there are mainly three types of classification of environmental interaction as shown in Figure 12. Type A shows accelerated fatigue crack growth due to environmental interactions even below K_{ISCC} which is the threshold required to initiate stress corrosion cracking. This process depends on the exposure time of crack tip to the environment. This occurs under cyclic loads and is a time dependent process. Decreasing the frequency of cyclic loading exposes the crack tip to environment for longer duration increasing the time period for chemical reactions at the crack tip enhancing the crack growth rate. Type B

stress dependent rather than time dependent. This process occurs only when the crack tip driving force K_{max} at the crack tip exceeds K_{ISCC} in an aggressive environment. The environmental contribution increases with an increase in the stress in this case. Type C is a combination of the other two types.

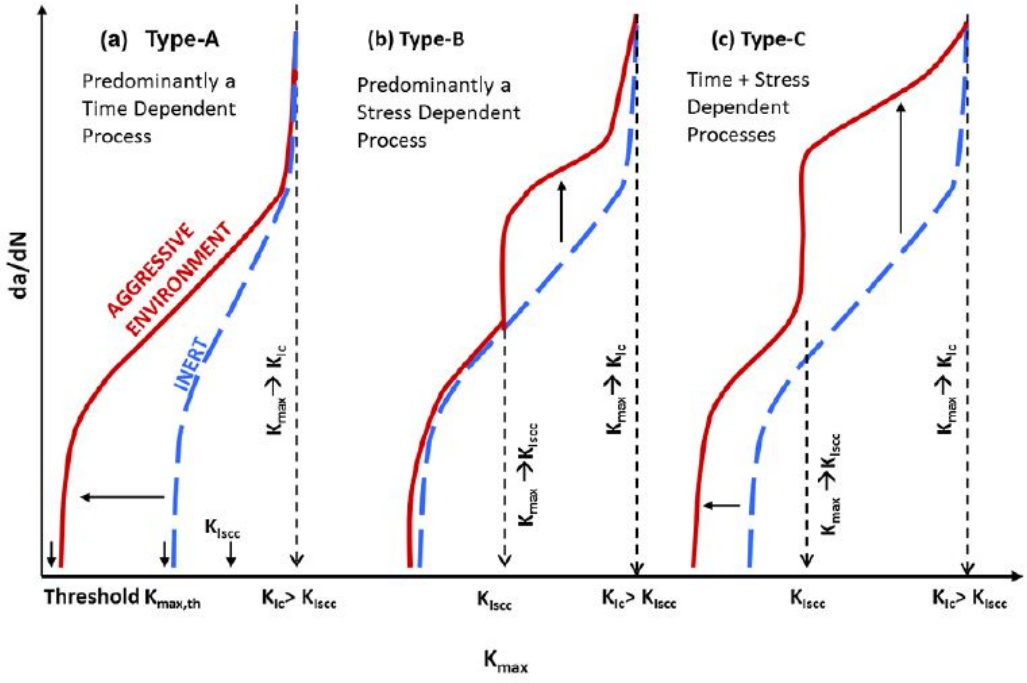

Figure 12. Classification of environmental interaction on fatigue crack growth based on da /dN vs ΔK curve [28]

For easiness of study of environmental interaction on fatigue crack growth, corrosion fatigue is divided into four main types in this paper as shown in Figure 13.Type A and Type B are stress independent. This occurs due to the synergistic action of cyclic loading and corrosive environment. Type A shows a retardation effect on fatigue crack growth in the near threshold region and merges with higher crack growth rates. This behavior can be observed in steels in dry environment such as dry hydrogen, dry argon and

so on. Type B shows an accelerating effect on the fatigue crack propagation which can be seen as a in Paris regime while the lower crack growth rates remain unaffected due to environmental interaction. This type of behavior can be observed in Aluminium alloys exposed to NaCl environment. In type C, corrosive environment accentuates the crack growth in the near threshold region. Ultra high strength steel in dry H2 shows this behavior for lower R ratios. Type D is stress dependent. The crack growth rates in aggressive environment are affected only above K_{ISCC} which is the threshold required for acceleration of crack growth under fatigue loading in aggressive environment. These types of behavior can occur in combinations as shown in Figure 14. Type B and Type C are the results of anodic dissolution and hydrogen embrittlement mechanisms due to the aggressive environment. Type D is due to the high applied tensile forces combined with adsorption of environmental species at the crack tip enhancing the crack growth. The possible reasons for Type A are not yet clear. Researches are still progressing to explain the possible mechanism for this type [27].

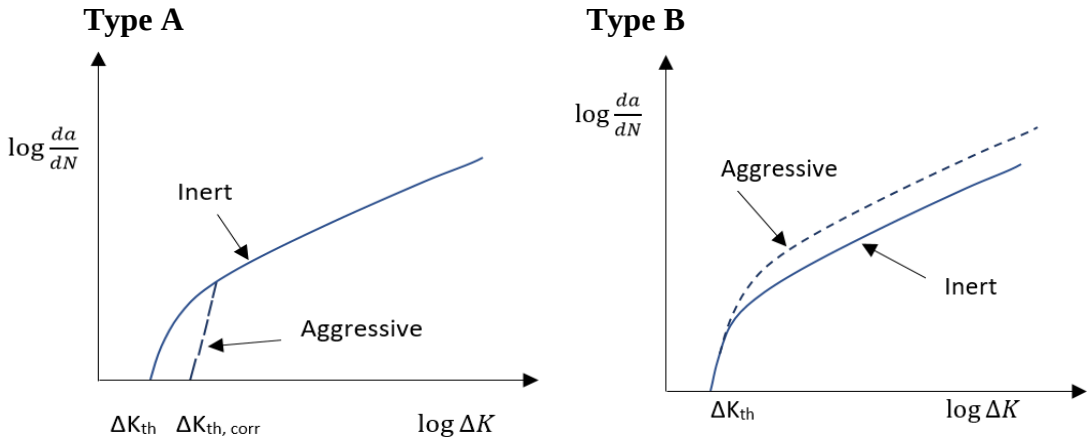

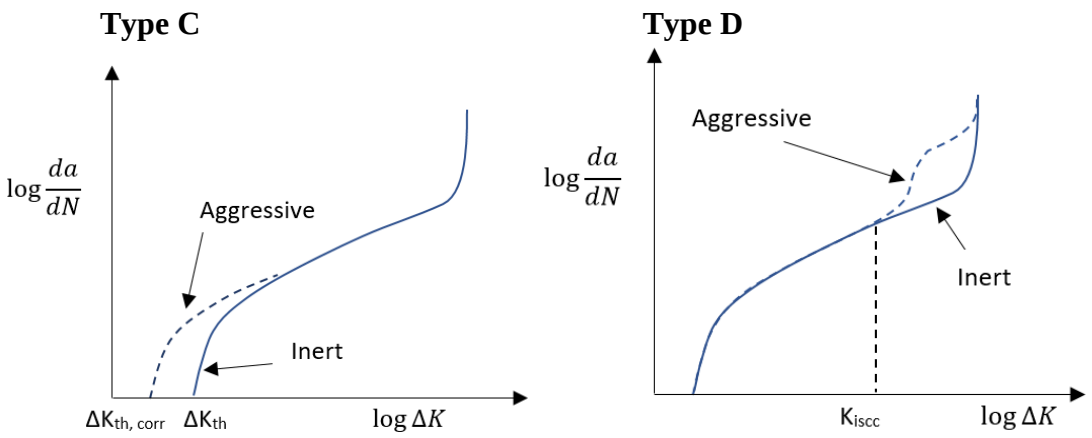

Figure 13. Types of Corrosion fatigue loading

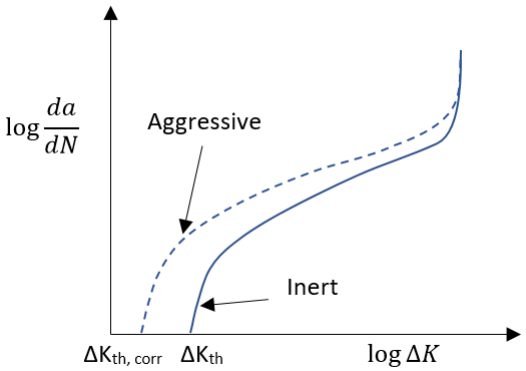

Figure 14. Combination of different types of corrosion fatigue loading

In the following sections, models are developed to predict the corrosion fatigue crack growth for Type A behavior in 1% NaCl and Type B behavior. These models are then validated against experimental data for various alloys.

3.2. Model development for the prediction of corrosion fatigue crack growth in Near threshold region for Type A behavior

In dry hydrogen environment, the threshold is found to be 14% higher than the threshold in air irrespective of R ratios [19]. The corrosion fatigue crack growth can be predicted by modifying the coefficient of threshold in the modified time scale model as

$$C_{th,corr} = \left\{ \frac{\Delta K_{eff} - (P_{corr} - Q_{corr}(1-\sqrt{(4\ \frac{r_f}{d_r})}))}{K_c - K_{max}} \right\}^n \qquad (31)$$

$$P_{corr} = k * P$$

$$Q_{corr} = k * Q$$

Where P and Q are the intercept and slope of ΔK_{th} vs R plot as given in section 2.4. The value of k is determined based on the increase in threshold in dry hydrogen environment compared to the threshold in air and is taken as 1.14.

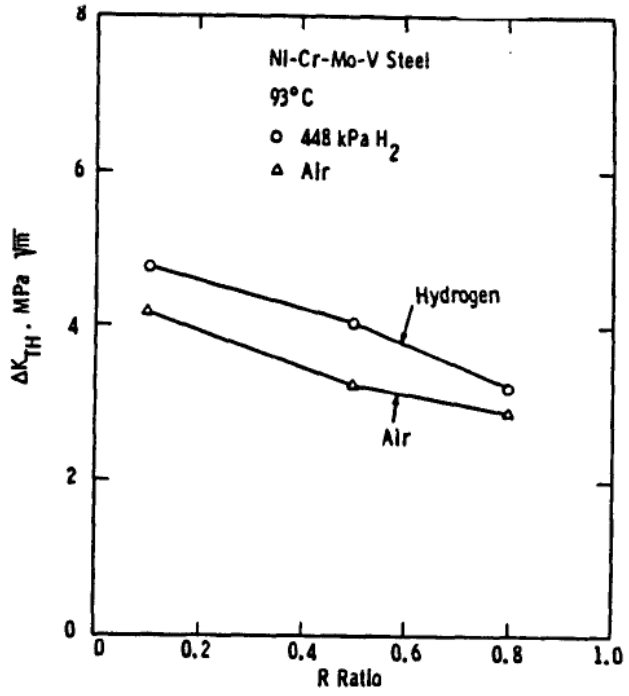

Figure 15. Effect of dry hydrogen on ΔKth for Ni-Cr-Mo-V steel at different R ratios [19]

3.3 Modeling for corrosion fatigue crack growth in Paris regime

The small time scale model predicts the fatigue crack growth behavior for various alloys in the Paris regime. The parameter A is the intercept that matches with the experimental data. Since there is a parallel shift in case of corrosion fatigue crack growth rate from the pure fatigue growth rate, the parameter A is modified in the small time scale model to account for this shift in the Paris region. The proposed modified small time scale model is

$$a = \mathrm{A_{corr}}\, K_{max}^{B} \sqrt{\delta} \qquad (32)$$

Experimental data were collected for the crack growth rate in pure fatigue and NaCl environment for various alloys to and studied. It was observed that for these alloys, the crack growth data showed a similar trend in the accelerating effect in the growth rate in NaCl environment. The modified A is proposed to be

$$\mathrm{A_{corr}} = \mathrm{kA} \qquad (33)$$

The value of k was determined empirically for different alloys as given in the table below.

The below table shows the values for k for various alloys.

Table 1. Values for k factor for Corrosion fatigue in 1% NaCl for various alloys

Material	**k**
Al 7075 –T6	4.2
Al 7075 – T7	3.7
HSLA 100	3.3
HSLA 80	2.2
2205 Duplex SS	1.5
Ti-6Al-4V	3.5

CHAPTER 4
MODEL VALIDATION AND DEMONSTRATION

4.1. Overview

This chapter gives an idea of the parameters used for the validation of the improvised small time scale model. The model is validated against the experimental data collected from the literature for constant amplitude loading. Since collecting the experimental data for variable amplitude loading is tedious and time consuming due to limited availability of crack growth rate data, the model is not validated for variable amplitude loading (VAL) but it is demonstrated for VAL. The table below shows the mechanical properties for different alloys tested.

Table 2. Mechanical properties of various alloys

Material	**E (GPa)**	**σ_y (MPa)**	**K_{IC} (MPa$\sqrt{m}$)**
HSLA 100	197.066	840	180
HSLA 80	197.066	650	180
Al 7075 – T7	72	435	20
Al 7075 – T6	71.7	503	20
300M – T650	205	1070	152
2205 Duplex SS	200	460	200
Ti-6Al-4V	113.763	758.423	76.918

The fitting parameters A and B are taken to be the intercept of Paris regime from experimental data collected. A and B shown below are taken at R = 0. Parameters P and Q are found from the linear curve of ΔK_{th} vs R.

Table 3. Fitting parameter values for various alloys

Material	**A**	**B**	**P**	**Q**
Al 7075 – T7	2.19077E-06	1.7638	2.9653	2.1194
Al 7075 – T6	1.75E-06	2.29	2.2732	1.3817
300M	1.4E-07	1.81	8.988	8.31
Ti-6Al-4V	9.75E-09	2.8318	3.5201	1.3712

The loading conditions used for the model validation are given as below:

Table 4. Loading condtions for prediction of fatigue and corrosion fatigue crack growth rate

Medium	**Loading Frequency, Hz**	**Concentration, %**
Air	10	-
NaCl	10	1%
Dry Hydrogen	10	

4.2. Model Validation for Constant Amplitude Loading (CAL)

Experimental data for crack growth rate per cycle as a function of stress intensity factor in ambient air is collected for various alloys such as 2205 duplex stainless steel, Al 7075, copper strengthened HSLA – 100, 300M - T650 high strength steel from literature to validate the small time scale fatigue model for near threshold and Paris regime for different R ratios. The experimental data is compared with the predicted data to verify the model. Small time scale corrosion fatigue model for Type A corrosion is validated by plotting the model predicted data against with the experimental data for 300M – T650 high strength steel in dry hydrogen. In order to validate the model for Type B corrosion, experimental fatigue crack growth data for various alloys such as HSLA – 100, Al 7075, duplex stainless steel are plotted.

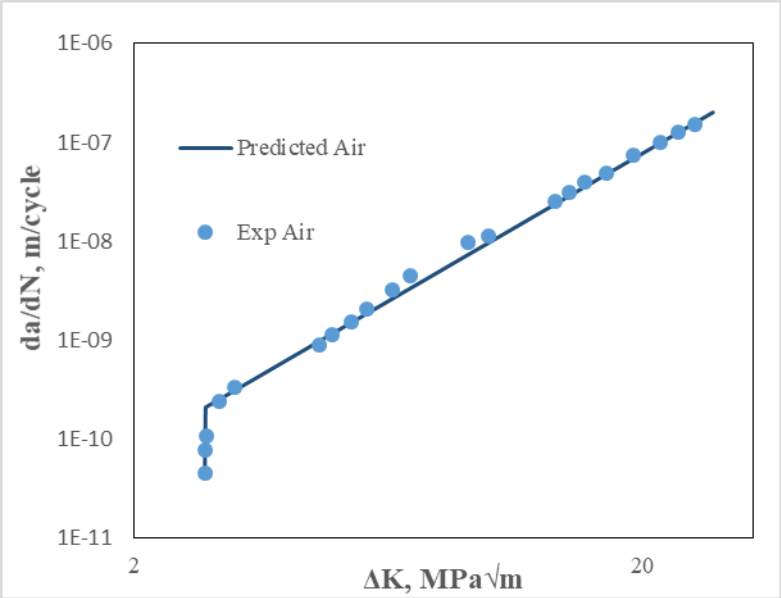

Figure 16. Log da/dN versus Log ΔK graph and predicted results for 300M in near threshold and Paris region at R = 0.7 [27]

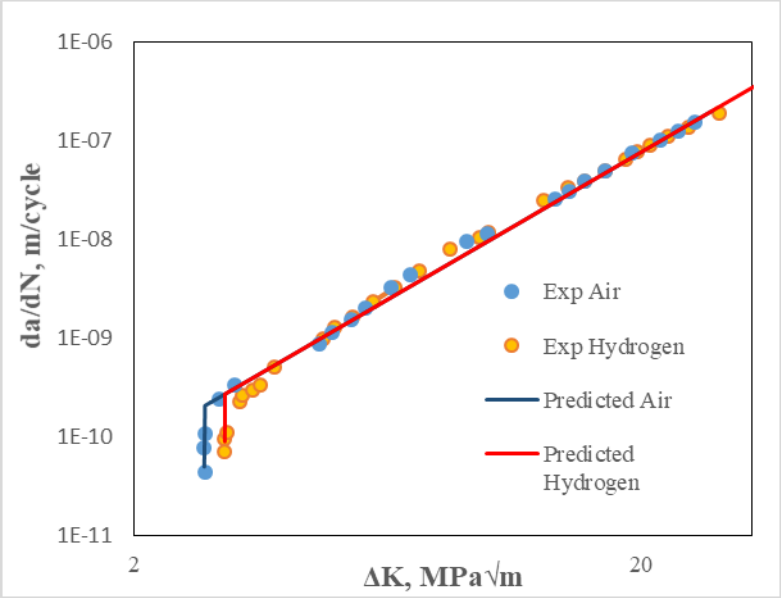

Figure 17. Log da/dN versus Log ΔK graph and predicted results for high strength 300-M at R = 0.7 [27]

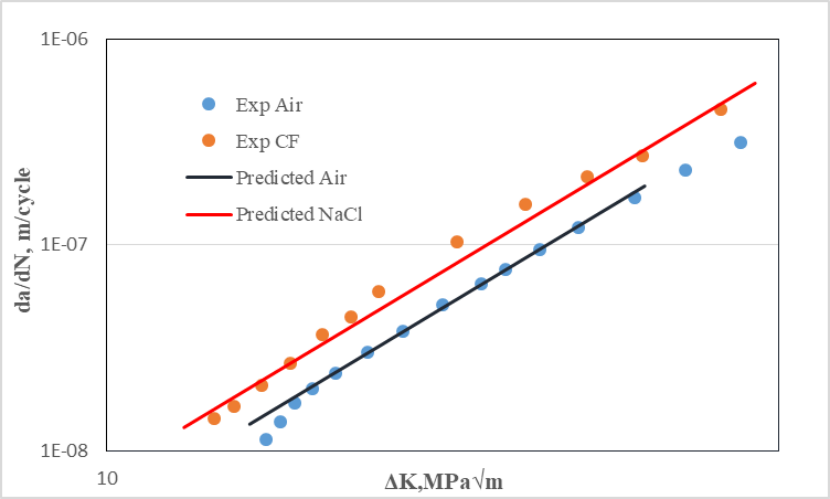

Figure 18. Log da/dN versus Log ΔK graph and predicted results for 2205 Duplex steel at R = 0.1 [30]

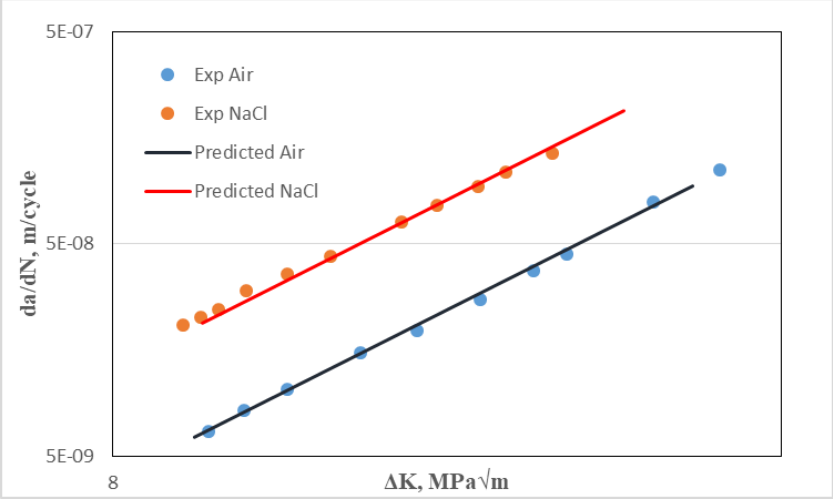

Figure 19. Log da/dN versus Log ΔK graph and predicted results for HSLA 100 at R = 0.5 [24]

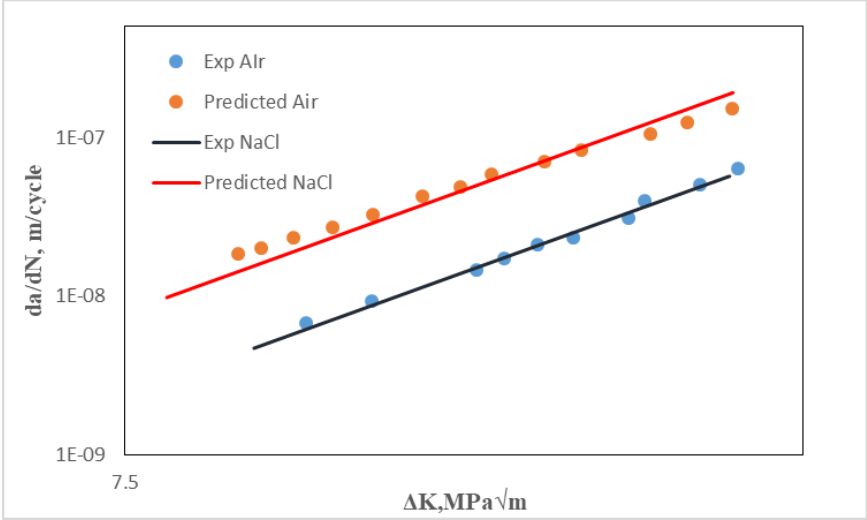

Figure 20. Log da/dN versus Log ΔK graph and predicted results for HSLA 100 at R = 0.1 [24]

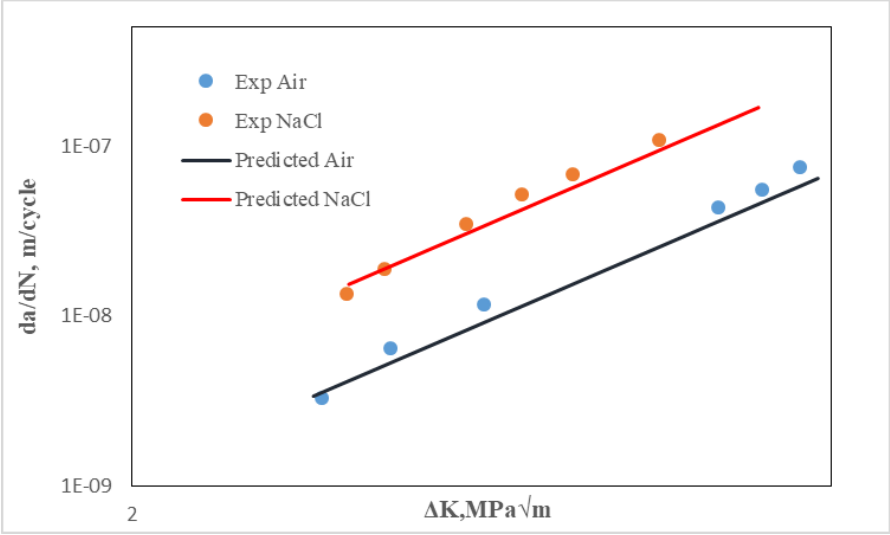

Figure 21. Log da/dN versus Log ΔK graph and predicted results for Al 7075-T651 at R = 0.1 [22]

4.3. Model Demonstration for Variable Amplitude Loading (VAL)

The model developed is applied to a random loading case to predict the fatigue crack growth rate and the corrosion fatigue crack growth rate. The below given figure is the random loading applied in 1% NaCl.

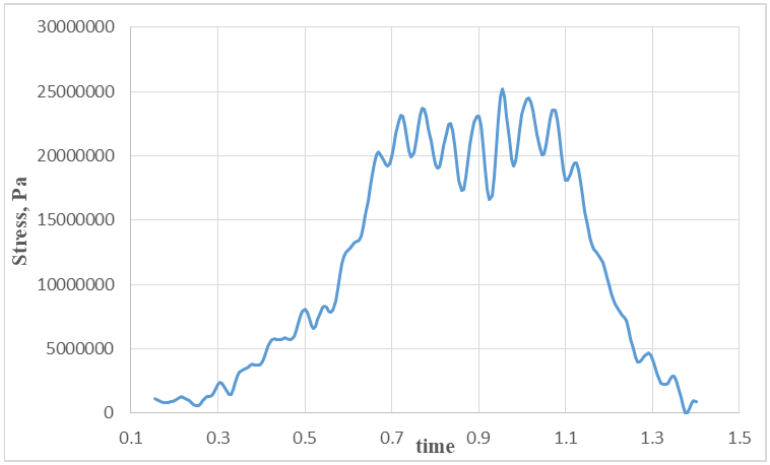

Figure 22. Applied random loading

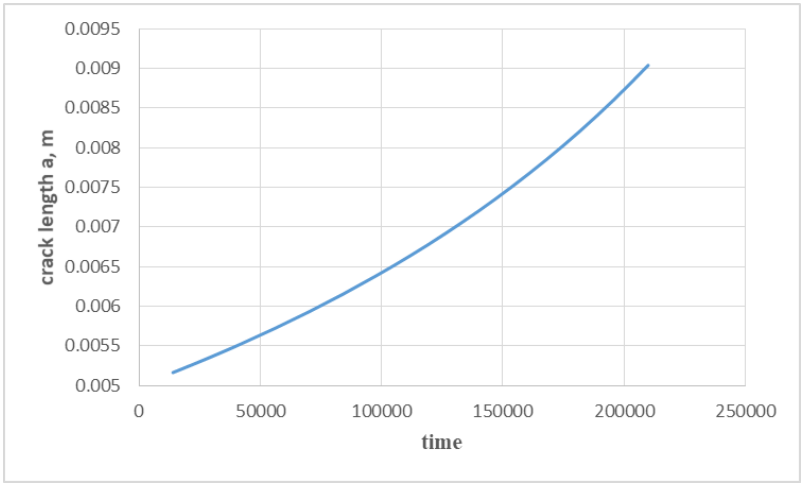

Figure 23. Fatigue crack growth rate for random variable loading

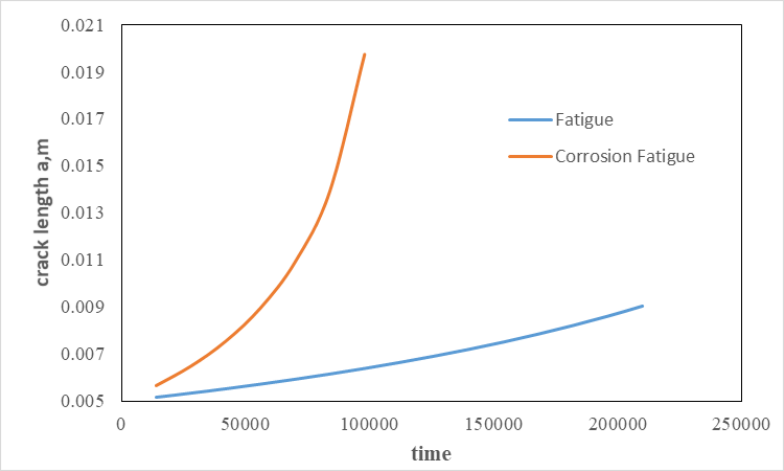

Figure 24. Crack length vs time graph for a variable amplitude loading in case of corrosion fatigue and mechanical fatigue

Figure 25 is the girder response data available for a day. This is an example of complex variable amplitude loading spectrum. The model is used to predict the length of the crack considering fatigue in air as well as the corrosion fatigue as given in Figure 26. 1% NaCl is the corrosive media considered.

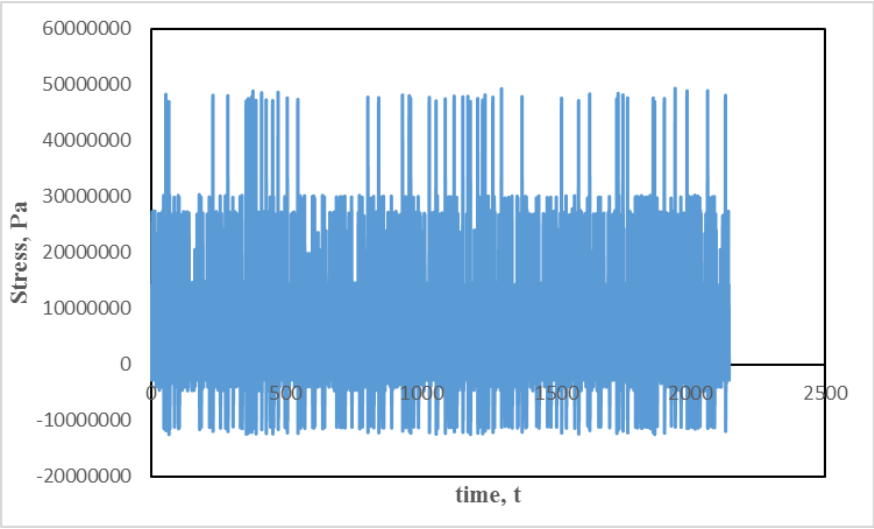

Figure 25: Girder response taken for a day (Stress vs time graph)

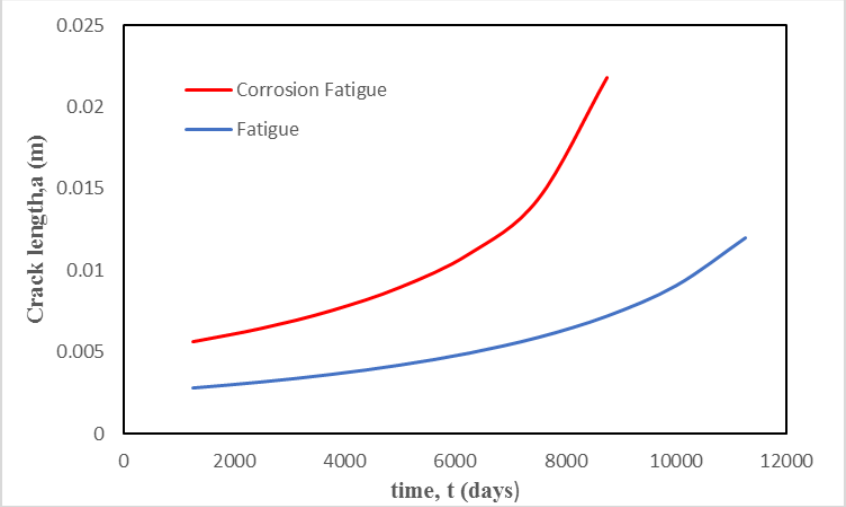

Figure 26: Predicted Crack length versus time for the Girder response

4.4. Results and Discussion

It can be seen that the model predicted data matches with the experimental data for constant amplitude loading. The model prediction for near threshold region however shows a slight variation in the near threshold region. The determination of exact stress intensity factor at which the crack growth rate changes from near threshold behavior to Paris regime is difficult. Materials show a smooth transition from near threshold to Paris regime. Since the model is developed for power law, the near threshold region is represented by a linear vertical curve and does not accommodate this smooth transition. The crack growth rate prediction for variable amplitude shows that consideration of environmental interactions is significant to avoid any premature failure of components.

CHAPTER 5
Conclusion and Future Work

5.1. Conclusion

An existing small time scale is modified to extend the prediction of crack growth in the near threshold as well as the unstable crack growth region along with the Paris region. A new coefficient C_{th} is introduced which is defined as a function of ΔK_{eff} and K_{max}. The crack closure effect seems to be predominant in the near threshold region. This is visible as a shift in the fatigue crack growth rate curve accompanied by a change in R in da/dN vs ΔK plot. In case of VAL, the crack closure level varies for sub cycles within a cycle as well for cycles and is included in the modified model as a function of the plastic zone sizes.

The effect of various corrosive environments such as NaCl and dry hydrogen on fatigue crack growth (FCG) was studied. It was observed that dry environments affect the FCG only at lower crack growth rates by a retardation in the growth rate. Salt-water environment speeds up the crack growth process. In this research, cases where this effect is visible only in the Paris region as a parallel shift are studied. More extensive data collection is required to study the effect of NaCl in near threshold region. The small time scale is improved to consider these two types of environmental interaction effect on FCG. Later on, the model predictions were compared with the experimental data to verify the applicability of model for various alloys.

5.2. Future Work

The following suggestions need to be investigated to consider the corrosion fatigue in a broader level.

- It was observed that the change in frequency of applied load has a significant effect mainly in the range of 0.1 Hz – 5 Hz. There are studies showing the significance of Rising time, RT over the frequency. This needs to be investigated thoroughly to understand the prominent factor in corrosion fatigue.
- It was observed that there is an effect of NaCl concentration on the corrosion fatigue crack growth (CFCG). From few studies, this effect was limited to the range 0.001% – 1%. The improved small time scale model can further be modified to account for this change in CFCG in under varying concentration of NaCl.
- Extensive data collection is required for the study of expedition of FCG in near threshold region under aggressive environment and the small time scale model needs to be improvised further to account for this effect.
- A model to predict the stress driven corrosion cracking may be developed in the future to be incorporated with the small time scale corrosion fatigue crack growth model. This occurs in specific alloy/environment interaction. The environments under which SCC may occur for the given alloy needs to be investigated initially and the threshold, K_{ISCC} required for various alloys to initiate SCC has to be determined.

REFERENCES

[1] Sadananda, K, Vasudevan, AK and Holtz, RL. 2001. Extension of the unified approach to fatigue crack gowth to environmental interactions. *International Journal of Fatigue* 23 (2001): S277 - S286.

[2] Paris, PC and Erdogan, F. 1963. A critical analyses of crack propagation laws. *Journal of Basic Engineering* 85 (1963) Transof ASME : 515.

[3] Forman, RG. 1967. Numerical analysis of crack propagation in cyclic loaded structure. *Journal of Basic Engineering* 89 (1967) Trans. ASME : 459.

[4] Nicholson, CE. 1973. Proceedings of Conference of Mechanics and Mechanism of Crack Growth. Cambridge,England.

[5] ELBER, W. 1970. The significance of crack closure, damage tolerance in aircraft structures. *ASTM STP* 486 (1971) : 230-242.

[6] Khan, AS. 1989. A new fatigue crack propagation model. Research Progress Report No. AMNE-89-2, DOD, OCALC/MMIRAE, Tinker AFB.

[7] Wheeler, Orville Eugene. 1972. Spectrum loading and crack growth. *Journal of basic engineering* 94 (1): 181–186.

[8] Newman, JC. 1982. Prediction of fatigue crack growth under variable-amplitude and spectrum loading using a closure model. *In Design of Fatigue and Fracture Resistant Structures*. ASTM International.

[9] Bannantine, Julie. 1990. Fundamentals of metal fatigue analysis. Prentice Hall, 1990 : 273.

[10] Lu, Zizi and Liu, Yongming. 2010. Small time scale fatigue crack growth analysis. *International Journal of Fatigue* 32 (2010) : 1306-1321.

[11] Zhang, Wei and Liu, Yongming. 2012. Investigation of incremental fatigue crack growth mechanisms using in situ SEM testing. *International Journal of Fatigue* 42 (2012) : 14-23.

[12] Liu, Yongming, Lu, Zizi and Zu, Jifeng . 2012. A simple analytical crack tip opening displacement approximation under random variable loadings" *International Journal of Fracture* 173 (2012):189-201.

[13] Venkatesan, Karthik Rajan. 2016. Subcycle fatigue crack growth formulation for constant and variable amplitude loading. Master's thesis, Arizona State University, Tempe, 2016.

[14] McClung, RC. 1990. Crack closure and plastic zone sizes in fatigue. *Fatigue Fract Eng Mater Struct* 14(4) (1990) : 455–68.

[15] Venkatesan, KR and Liu, Yongming. 2017. Subcycle fatigue crack growth formulation under positive and negative stress ratios. *Engng Fract Mech* (2017).

[16] Gangloff, RP and Ives, MB. 1990. Corrosion fatigue crack propagation in metals. *Environment-Induced Cracking of Metals*. R.P. Gangloff and, eds., NACE, Houston, TX : 55-109.

[17] Gangloff, RP and Wei, RP. 1977. *MTA,* 8 (1977) 1043-1053.

[18] Speidel, MO. 1979. Stress corrosion and corrosion fatigue crack growth in aluminum alloys. *Stress Corrosion Research*. H. Arup and R.N. Parkins,eds., Sijthoff & Noordhoff, Alphen aan den Rijn, The Netherlands : 117- 176.

[19] Ritchie, RO, Suresh, S and Liaw P K. 1981. A comparison of environmentally influenced near threshold fatigue crack growth behaviour in high and lower strength steels at conventional frequencies. Proceedings of the Engineering Foundation Conference on *Fatigue and Corrosion Fatigue upto Ultrasonic Frequencies* October 1981.

[20] Wei, RP and Landes, JD. 1969. *Matls. Res. Stds* 9 (1969) : 25 – 28.

[21] Stewart, AT. 2006. The influence of environment and stress ratio on fatigue crack growth at near threshold stress intensities in low alloy steels. *Engineering Fracture Mechanics* Vol. 13 (2006) : 463-478.

[22] Pao, PS and Holtz, RL. 2014. Corrosion fatigue cracking in Al 7075 alloys. Naval Research Laboratory,Washington DC.

[23] Menan, Frederic and Henaff, Gilbert. 2010. Synergistic action of fatigue and corrosion during crack growth in the 2024 aluminium alloy. *Procedia Engineering* 2 (2010) : 1441–1450

[24] Sivaprasad, S, Tarafder, S, Ranganath, VR, Tarafder, M and Ray, KK. 2005. Corrosion fatigue crack growth behaiour of naval steels. *Corrosion Science* 48 (2006) : 1996–2013.

[25] Standard test method for measurement of fatigue crack growth rates, ASTM E-647, 2003 : 615-657.

[26] Jordon, JB, Newman, JC Jr., Xue, Y and Horstemeyer, MF.2006. Near threshold fatigue crack growth in 7075-T651 aluminum alloy. *Proceedings of the 2006 SEM Annual Conference and Exposition on Experimental and Applied Mechanics* (2006), Saint Louis, MO: Society for Experimental Mechanics Inc. *4* : 1742-1750.

[27] Ritchie, RO. 1977. Near-threshold fatigue crack propagation in ultra-high strength steel: influence of load ratio and cyclic strength. *Journal of Engineering Materials and Technology* (1997), ASME.

[28] Sadananda, Kuntimaddi and Vasudevan Asuri. 2015. Crack growth behavior of 4340 steel under corrosion and corrosion fatigue conditions. *Corrosion review* (2015) , DOI: 10.1515/corrrev-2015-0034.

[29] Green, AM and Knott, JF. 1989. Effects of environment and frequency on the long fatigue crack growth of aluminum alloy 7475. *Advances in Fracture Research*. K. Salama, K. Ravi-Chandar, D.M.R. Taplin, and R.P. Rao, eds., Pergamon Press, Oxford, UK : 1747-1756.

[30] Bin ,Yang, Ji, Chen, Yue, Geng, Xiao, Cui and Wanglin, Gui. Corrosion Fatigue Crack Propagation Behavior of 2205 Duplex Stainless Steel in Aqueous Medium. Corrosion Science and Protection Technology[J], 2018, 30(2): 182-186 doi:10.11903/1002.6495.2017.084